American Mineralogist, Volume 97, pages 1828–1833, 2012

Blue spinel crystals in the $MgAl_2O_4$-$CoAl_2O_4$ series: Part I. Flux growth and chemical characterization

Veronica D'Ippolito,[1] Giovanni B. Andreozzi,[1,*] Ferdinando Bosi,[1] and Ulf Hålenius[2]

[1]Dipartimento di Scienze della Terra, Sapienza Università di Roma, Piazzale Aldo Moro 5, I-00185 Roma, Italy
[2]Department of Mineralogy, Swedish Museum of Natural History, SE-10405 Stockholm, Sweden

Abstract

Natural blue Co-bearing spinel crystals are rare and actively sought as gemstones, while synthetic blue Co-bearing spinel powders are largely used as ceramic pigments. High-quality spinel single crystals with compositions closely corresponding to the solid-solution series spinel sensu stricto ($MgAl_2O_4$)-cobalt spinel ($CoAl_2O_4$) were produced by flux growth method, with $Na_2B_4O_7$ as flux. Low-cooling rates (2 °C/h) and linear temperature profiles were applied in the thermal interval 1200–800 °C, followed by rapid cooling. Thermal runs were performed in reducing atmosphere (f_{O_2} 10^{-8}–10^{-15} bars) created by a continuous flow of a CO_2:H_2 mix with a ratio of 100:4 (cm^3/min). Ten experiments were successfully carried out and hundreds of inclusion-free gem-quality single crystals (up to 1 mm large) were produced in each of them, sometimes together with crusty aggregates and microcrystalline powder. Selected crystals were investigated by SEM/EDS X-ray mapping to check for compositional homogeneity and by electron-microprobe analysis to obtain the chemical formula. Crystals were found to be chemically homogeneous and entirely representing the $MgAl_2O_4$-$CoAl_2O_4$ solid-solution series, with the latter component ranging from 7 to 100%. With increasing Co^{2+} contents, the crystals vary in color from light blue to intensely dark blue in daylight. The unit-cell parameter *a* increases from 8.084 to 8.105 Å along the solid-solution series, and the observed increase is determined more by the inversion degree than by the variation in Co contents. The composition of crystal products does not correspond to the composition of the starting oxide mixture, being cobalt enriched in the crystals. A tentative explanation of this behavior is suggested by considering possible ionic potential as well crystal field stabilization effects.

Keywords: Cobalt spinel, $CoAl_2O_4$, single crystal, flux growth, electron microanalysis

Introduction

Co-bearing spinels are very rare in nature, but are actively sought as gemstones due to their vivid, high-purity blue color that makes them more precious than sapphires. Previous studies evidenced small amounts of cobalt (CoO = 1 wt%) in natural gems of Sri Lanka (Shigley and Stockton 1984) and in a sample from the island of Samos (Taran et al. 2009). Although the cobalt contents were very low, these natural Co-bearing spinel crystals showed light and fancy blue colors. Up to a few decades ago cobalt was considered a coloring agent only of synthetic blue spinel, whereas the blue color in natural spinel was attributed solely to iron. However, Shigley and Stockton (1984) demonstrated that both cobalt and iron are capable of producing blue colors in materials, and considerably less cobalt than iron is required to produce an equally intense blue. Besides the above mentioned natural Co-poor spinel crystals, the only reported natural occurrence of a Co-rich spinel (CoO ≤ 22.8 wt%) is a very small crystal (~200 μm large) included in a gem-quality blue sapphire from Bo Phloi, Thailand (reported as Bo Ploi in gemological literature), occurring in alluvial/eluvial deposits near basaltic outcrops (Guo et al. 1994).

Synthetic $CoAl_2O_4$ spinel is a high-temperature oxide (melting point of 1955 °C), and it is the most stable compound of a family of spinel-structured oxides obtained from Co_3O_4 at progressive increase of Al contents (Tielens et al. 2006, 2009). From an optical point of view, the increase of Al results in the transition from black Co_3O_4 to dark green Co_2AlO_4, bright blue $CoAl_2O_4$, and white $Al_{8/3}O_4$, that is, γ-Al_2O_3. These color changes are functions of both the oxidation states and the structural position of the cobalt cations. The black color is caused by total absorption of visible light due to the interactions between Co^{2+} and Co^{3+} (i.e., comparable to Fe^{2+}-Fe^{3+} in magnetite), the dark green color is ascribed to electronic transitions in Co^{3+} in octahedral coordination, and the bright blue color results from electronic transitions in Co^{2+} in tetrahedral coordination (Burns 1993; Fernández and Pablo 2002; Tielens et al. 2006, 2009; Kurajica et al. 2011). Bright blue synthetic $CoAl_2O_4$ is commercially well known as Thenard's blue and has been extensively used, since the discovery of its industrial synthesis route in 1802, as a pigment (classified with the DCMA number 13-26-2) for the coloration of ceramics, glazes, porcelain enamels, glass, paint, fibers, paper, cement, rubber, plastics, and cosmetics. Cobalt-bearing pigments, commonly Co-spinel and Co-olivine, are the most efficient and widely used blue ceramic pigments, but the spinel is strongly preferred to olivine since a navy blue color can be obtained with strongly reduced CoO content (42 wt% in $CoAl_2O_4$ against 71 wt% in Co_2SiO_4), besides some differences

* E-mail: gianni.andreozzi@uniroma1.it

0003-004X/12/1112–1828$05.00/DOI: http://dx.doi.org/10.2138/am.2012.4138

in color saturation (Eppler and Eppler 2000). In addition to pigment industry, cobalt-aluminate and iron-manganite spinels have been successfully used for heterogeneous catalysis such as NO_x reduction or the CO_2 reforming of methane (Hou and Yashima 2004; Fierro et al. 2005).

Spinels are double oxides with AB_2O_4 general formula (space group $Fd\bar{3}m$) in which A and B cations of variable valence may occupy the tetrahedrally and octahedrally coordinated interstices of the densely packed oxygen atoms array. In spinels containing divalent (A) and trivalent (B) cations, two extreme site populations are possible: the normal one in which divalent cations are located at the tetrahedrally coordinated (T) sites and trivalent cations are at the octahedrally coordinated (M) sites [e.g., spinel sensu stricto $MgAl_2O_4$, $^{T}(Mg)^{M}(Al)_2O_4$]; the inverse one in which one half of the trivalent cations occupies the T sites and the other half occupies the M sites together with divalent cations [e.g., magnesioferrite $MgFe_2O_4$, $^{T}(Fe^{3+})^{M}(MgFe^{3+})O_4$]. Between these two ordered extremes, intermediate disordered site populations are possible, which are characterized by the so-called inversion parameter, *i*, variable from zero (normal) to 1 (inverse): $^{T}(A_{1-i}B_i)^{M}(B_{2-i}A_i)_2O_4$. In natural as well as in synthetic spinels, the inversion parameter variation is a function of both composition and thermal history (Andreozzi et al. 2000, 2001; Andreozzi and Princivalle 2002; Bosi et al. 2004, 2007). As spinel systems are structurally simple but compositionally highly flexible, a large number of crystal-chemical studies have been performed on synthetic materials of well-defined compositions, with the objective to model its physical properties. As for example, $CoAl_2O_4$ has been extensively synthesized by several methods: sol-gel method (Sales et al. 1997; Areán et al. 1999), coprecipitation method (Chokkaram et al. 1997; Rangappa et al. 2007), polymeric precursor method (Cho and Kakihana 1999; Gama et al. 2009), solid-state reactions (Chemlal et al. 2000; Melo et al. 2003; Suzuki et al. 2007), combustion synthesis (Mimani and Ghosh 2000; Li et al. 2003), hydrothermal synthesis (Chen et al. 2003), complexation method (Wang et al. 2006; Mindru et al. 2010) floating-zone technique (Maljuk et al. 2009). The solid solution $(Co,Mg)Al_2O_4$ was explored by Angeletti et al. (1977), by calcination of alumina powder soaked in cobalt nitrate solution to 1200 °C. They obtained six compounds, mainly consisting of powder or nanosized particles of cobalt spinel. The chemical composition of synthetic powder materials is difficult to characterize accurately, especially when transition elements with more than one oxidation state are present. An alternative approach is to synthesize large single crystals, which offer the potential for high-accuracy material characterization.

In the present study, a flux growth method was used and experimental conditions were optimized to obtain high-quality single crystals of spinel with compositions corresponding to the solid-solution series $MgAl_2O_4$-$CoAl_2O_4$. The materials obtained have been characterized via scanning electron microscope (SEM), electron microprobe (EMP), and X-ray diffraction (XRD).

Experimental methods

Crystal synthesis

Ten experiments were carried out along the $MgAl_2O_4$-$CoAl_2O_4$ solid-solution series at the Department of Earth Sciences, Sapienza University of Rome. The starting materials consisted of analytical MgO, Al_2O_3, and CoO powders, which were dehydrated and dried at 1000 °C for 12 h, before being mixed with $Na_2B_4O_7$, used as flux compound. $Na_2B_4O_7$ was chosen because of its low melting point (742.5 °C), the low-energy barriers to crystal growth in the borate flux and its absence of interaction with spinel compositions. About 5 g of starting material were thoroughly ground and mixed under acetone in an agate mortar and then transferred to a 10 mL yttrium-stabilized Pt/Au (5%) crucible, covered by a platinum lid. The crucible was suspended inside an ENTECH vertical furnace equipped with a multi-step temperature controller and an oxygen fugacity control system, which uses a binary gas mixture (CO_2-H_2). Continuous flow of the two gases was kept constant in the ratio of 100:4 (cm^3/min) by TYLAN flow controllers to obtain a reducing condition, with the oxygen fugacity ranging from 10^{-8} to 10^{-15} bars when temperature is decreased from 1200 to 800 °C, respectively. The best flux/nutrients ratio (F/N) of each composition was determined by trial and error as no literature data were found, and F/N changed from 1.50 to 1.40 (Table 1). Thermal runs consisted of a rather steep increment in temperature up to 1200 °C, after which the temperature was kept constant for 24 h (for complete dissolution and homogenization of the oxide mixture) and subsequently decreased slowly to 800 °C at 2 °C/h cooling rate (as a first trial, the CoAl0.5 run was cooled down at 4 °C/h, but results were not completely satisfactory in terms of crystal quality, so that cooling time was doubled for subsequent runs). Shutting off the power to the heating elements ended thermal runs, and the material was rapidly cooled down to room temperature.

The products of each of the 10 experiments consisted of an intergrowth network of elongated, prismatic cobalt-magnesium borate crystals and octahedral spinel crystals embedded in minor sodium borate glass. By dissolving the glass phase and most of the borate crystals in warm and dilute HCl (10%) solution, the run products were reduced to euhedral and/or subhedral octahedra of spinels of various sizes (Table 1).

Single-crystal XRD

High-quality crystals were selected for structural investigation using a Bruker KAPPA APEX II single-crystal diffractometer equipped with a CCD area detector. Full experimental details are reported in Bosi et al. (2012, this issue). Final unit-cell parameters were refined by using the Bruker AXS SAINT program from ca. 2300 recorded reflections with $I > 10\,\sigma_I$ in the range $8° < 2\theta < 90°$, and results are reported in Table 2.

EMP analysis

After X-ray data collection, the same crystals were mounted on glass slides, polished, and carbon coated for electron microprobe analysis (at CNR-IGAG lab c/o Sapienza University of Rome) by wavelength-dispersive X-ray spectrometry (WDS) on a Cameca-Camebax SX50 instrument operating at an accelerating

Table 1. Flux grown spinels of the $MgAl_2O_4$-$CoAl_2O_4$ series: molar proportions of starting oxide mixture, flux to nutrient ratio (F/N), and experimental conditions

Run	CoAl0.5	CoAl1	CoAl10	CoAl14	CoAl20	CoAl34	CoAl45	CoAl50*	CoAl67	CoAl100
MgO	1.20	1.20	1.15	0.96	0.95	0.76	0.65	0.60	0.43	–
CoO	0.05	0.01	0.10	0.14	0.20	0.34	0.45	0.50	0.67	1.00
Al_2O_3	1.00	1.00	1.00	1.00	1.00	1.00	1.00	1.00	1.00	1.00
F/N	1.50	1.50	1.50	1.50	1.50	1.45	1.45	1.45	1.45	1.40
T range (°C)	1200–800	1200–800	1200–800	1200–800	1200–800	1200–800	1200–800	1200–800	1200–800	1200–800
Cool. range (°C/h)	4	2	2	2	2	2	2	2	2	2
CO_2:H_2 (cm^3/min)	100:4	100:4	100:4	100:4	100:4	100:4	100:4	100:4	100:4	100:4
Yield (g)	0.80	0.85	1.85	1.80	1.90	~1.80	~1.70	1.90	~1.20	~1.75
Mean size (μm)	300	300	500	500	500	500	500	500	500	500

* Accidental quenching happened before the end of the slow cooling path.

TABLE 2. Average chemical composition and unit-cell parameter (*a*) of synthetic crystals belonging to the $MgAl_2O_4$-$CoAl_2O_4$ series

Sample	CoAl0.5	CoAl1	CoAl10	CoAl14	CoAl20	CoAl34	CoAl45	CoAl50	CoAl67	CoAl100
MgO	25.9(7)	25.2(1)	24.2(9)	20.0(1)	17.8(7)	13.1(5)	10.5(4)	9.1(1)	6.0(1)	–
CoO	3.6(5)	4.4(1)	5.3(1)	12.4(3)	16.9(3)	22.4(5)	27.2(6)	29.0(2)	34.0(1)	43.1(3)
Al_2O_3	70.5(4)	70.3(3)	70.2(3)	67.1(3)	66.2(3)	63.8(2)	62.3(3)	62.0(2)	59.3(6)	57.3(2)
Total	100.0	99.9	99.7	99.5	100.9	99.3	100.0	100.1	99.3	100.4
Cations on basis of 4 oxygen anions										
Mg	0.929(4)	0.908(3)	0.878(4)	0.753(4)	0.676(4)	0.520(4)	0.424(6)	0.369(3)	0.252(5)	–
Co^{2+}	0.069(1)	0.085(2)	0.103(3)	0.251(3)	0.344(3)	0.478(4)	0.590(14)	0.635(4)	0.768(4)	1.017(5)
Al	2.002(4)	2.005(4)	2.012(5)	1.997(5)	1.986(4)	2.001(5)	1.991(13)	1.997(2)	1.986(4)	1.989(5)
Total	3.000	2.998	2.993	3.001	3.006	2.999	3.005	3.001	3.006	3.006
a (Å)	8.0851(3)	8.0848(4)	8.0840(3)	8.0875(4)	8.0902(3)	8.0914(4)	8.0943(3)	8.0957(3)	8.1010(5)	8.1047(4)

potential of 15 kV and a sample current of 15 nA, with an incident beam size of ~1 µm. No less than 5 spot analyses for each sample were performed to obtain the average chemical composition and a preliminary estimation of the compositional homogeneity (Table 2). Synthetic standards used were periclase (MgO), corundum (Al_2O_3), and metallic Co. A synthetic $MgAl_2O_4$ spinel single crystal, produced and fully characterized by Andreozzi et al. (2000), served as a reference material. A PAP-CAMECA program was used to convert X-ray counts into weight percentages of the corresponding oxides.

X-ray mapping technique in SEM/EDS analysis

Compositional homogeneity was further investigated by SEM and demonstrated by image analysis coupled with energy-dispersive spectrometry (EDS) analysis using color coding to depict the 2D spatial distribution of the characteristic energy emission from respective elements present in the samples. All the samples were carbon coated and analyzed at Earth Sciences Department, Sapienza University of Rome, by a SEM/EDS FEI Quanta 400 instrument operating at an accelerating voltage of 30 kV, a specimen tilt of 0°, a working distance of 9.7 mm and a magnification of 520×.

RESULTS AND DISCUSSION

Conditions adopted during flux growth proved to be well optimized as demonstrated by the large number of spinel single crystals obtained from every experimental run. Apart from the first tentative run (CoAl0.5, see experimental section), all subsequent runs had the same thermal path and cooling rate. Crystals were formed in the range between 1200 and 800 °C, with an exception being sample CoAl50, which by accident was quenched before the end of the slow cooling stage. The unintentional breaking of the wire that holds the crucible in the vertical furnace resulted in a rapid cooling of the crystals of this run in the middle of the growth process. In spite of this, good quality spinel crystals were retrieved and the quenching temperature was estimated to be approximately 1000 °C. Due to this difference in thermal history, it may be expected that the structural/physical properties of sample CoAl50 will differ from the general trends identified for the majority of the other samples.

Crystals obtained at the end of each experimental run were inclusion-free, regular octahedra sized up to 1.2 mm in diameter, variable in color from light blue to intensely dark blue as a function of chemical composition (Fig. 1). With rising total cobalt content the saturation of the vivid blue color increases but no shift in color hue is observed along the series. In contrast, distinct color shifts were observed by the naked eye (and confirmed by optical absorption spectroscopy) in Fe^{2+}- and Cr^{3+}-bearing spinel solid-solution series previously synthesized (Hålenius et al. 2002, 2010). Besides large single crystals, solid crusty aggregates and loose microcrystalline powder were also obtained from most of the experiments and usually retrieved from the bottom of the Pt-crucible. SEM inspection showed that both the crusts and the powder consist of smaller spinel crystals (probably second

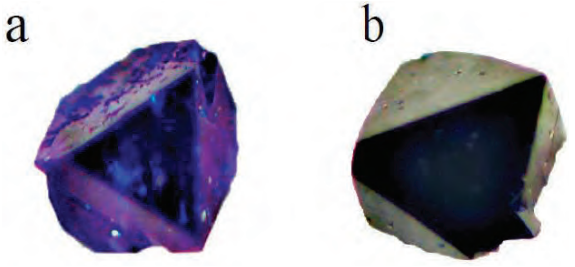

FIGURE 1. Photomicrographs of selected synthetic spinel single crystals: (**a**) sample CoAl1; (**b**) CoAl20. Crystal size is approximately 300 µm.

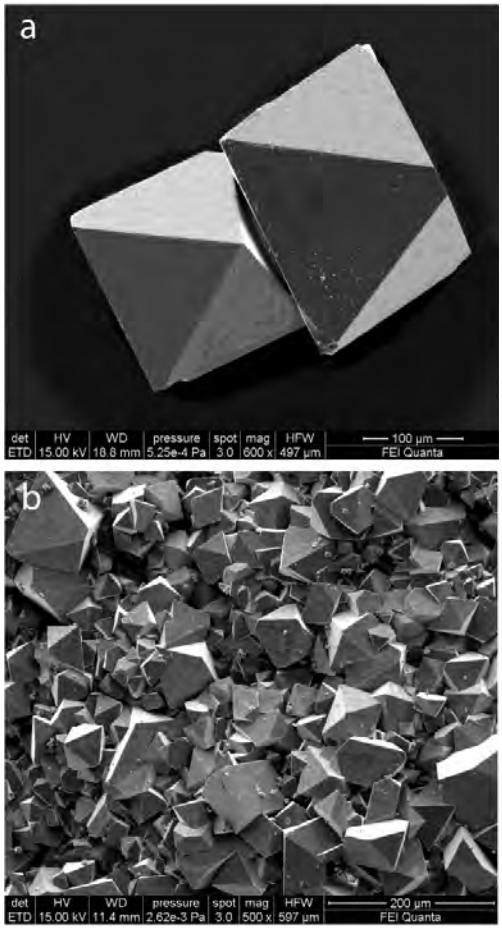

FIGURE 2. SEM images of selected small spinel samples retrieved at the bottom of the Pt crucible: (**a**) single crystals (magnification 600×); (**b**) crusty aggregates (magnification 500×).

generation or influenced by the interaction with the crucible walls) with octahedral shape and sharp edges (Fig. 2).

Chemical characterization via EMP confirmed that both large and small crystals belong to the $(Mg,Co)Al_2O_4$ spinel series, without evidence of other phases. This is an experimental confirmation of what was expected on the basis of ab initio calculations by Tielens et al. (2009), who showed the larger thermodynamic stability of the $CoAl_2O_4$ phase with respect to other $(Co,Al)_3O_4$ phases. These authors also predicted that the formation process of $CoAl_2O_4$ is largely exothermic and consequently this phase is highly stable with respect to decomposition. The present spinels satisfactorily represent the whole $MgAl_2O_4$-$CoAl_2O_4$ solid solution as their $CoAl_2O_4$ component ranges from 7 to 100 mol% (Table 2). Cation sums are in excellent agreement with the expected value required from spinel stoichiometry and this is a good indication against any presence of Co^{3+}. The absence of Co^{3+} in our samples was expected due to the strongly reducing conditions imposed during crystal growth, and it has been also confirmed by UV-VIS-NIR spectroscopy and crystal structure refinements (Bosi et al. 2012, this issue). Moreover, EMP spot analyses indicate compositional homogeneity within a single crystal, further evidenced by SEM/EDS X-ray mapping, which displays for all samples the lack of chemical zoning via uniform spatial distribution of Co (Fig. 3). In contrast, in Cr-bearing synthetic spinels previously produced a strong Cr enrichment was observed in the core region, especially in samples with low nominal Cr-contents (Hålenius et al. 2010).

The unit-cell parameter *a* of the present $(Mg,Co)Al_2O_4$ synthetic spinel crystals increases from 8.084 to 8.105 Å along the solid-solution series (Table 2). In literature there are many X-ray powder diffraction investigations on the end-member $CoAl_2O_4$ (JCPDS file no. 44-0160), all of them with an *a*-value close to 8.105 Å (Fig. 4). To our knowledge only Angeletti et al. (1977) addressed the entire $MgAl_2O_4$-$CoAl_2O_4$ series, and the values of the unit-cell parameter they obtained are in line with those measured here. The observed linear increase of the *a* parameter is seemingly due to the increase of the $CoAl_2O_4$ component. However, this is a premature and misleading conclusion because it is well known that structural changes in spinels may depend on both chemical composition and inversion parameter, which in turn is a function of thermal history (O'Neill and Navrotsky 1984; O'Neill and Dollase 1994; Harrison et al. 1998; Andreozzi et al. 2000, 2001; Andreozzi and Lucchesi 2002; Quintiliani et al. 2011). In the present case, the values of unit-cell parameter for the $MgAl_2O_4$-$CoAl_2O_4$ series at $i = 0$ were calculated from cation-to-oxygen distances refined in Bosi et al. (2012, this issue), which are consistent with those reported in Lavina et al. (2002). Results show that the contribution of the inversion degree strongly affects the unit-cell parameter, which at $i = 0$ is quite insensitive to the substitution of Co for Mg (Fig. 4). The trend obtained for the present samples (which experienced a closure temperature of ca. 800 °C) and the trend calculated for $i = 0$ cross each other close to the composition of 60% $CoAl_2O_4$, that is almost coincident with the sample CoAl50, and this intercept is expected to be temperature-invariant. This coincidence explains why the sample CoAl50 (which experienced a closure temperature distinctly higher than the others) shows a unit-cell parameter in line with the general trend.

If a comparison between the composition of starting oxide mixture (reagents) and the composition of crystalline materials (products) is made, it is evident that the $CoAl_2O_4$ component of our products does not show a linear relationship with the analogous component of the reagents, but rather a distinct symmetrical deviation (Fig. 5). In particular, the difference between products and reagents is zero at the two end-members and reaches a maximum value of ca. 14% (in terms of $CoAl_2O_4$ component expressed in mol%) for the samples in the central part of the series (CoAl34, CoAl45, and CoAl50), reflecting a concentration of cobalt into the crystalline phase. It is noteworthy that opposite behavior was observed in the previously synthesized $MgAl_2O_4$-$FeAl_2O_4$ and $MgAl_2O_4$-$MnAl_2O_4$ solid-solution series (Andreozzi and Lucchesi 2002; Hålenius et al. 2011). A plot of corresponding data for those two binary systems shows a marked depletion of their transition metal component in the crystal products with

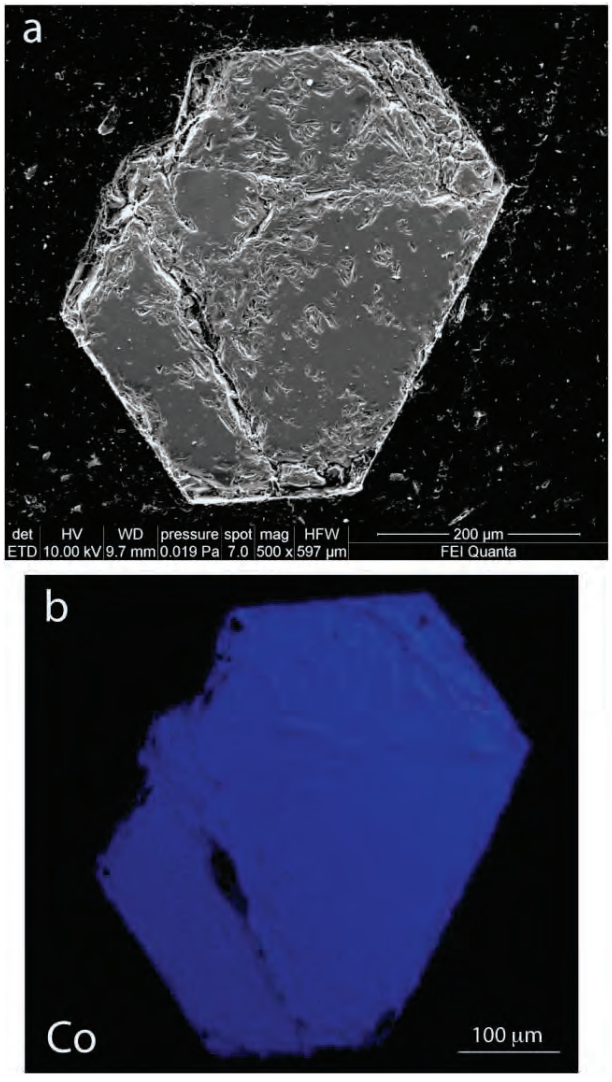

FIGURE 3. SEM/EDS X-ray map of CoAl67 sample: (**a**) SEM image of a polished crystal; (**b**) uniform spatial distribution of Co concentration (identified by the constant saturation of blue color).

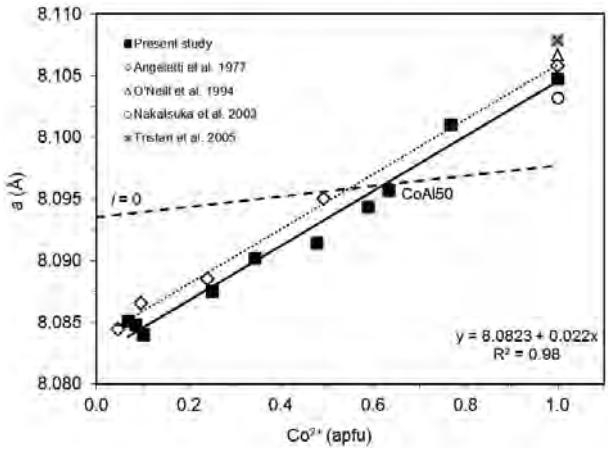

FIGURE 4. Unit-cell parameter *a* against Co^{2+} content in $MgAl_2O_4$-$CoAl_2O_4$ solid-solution series. Size of the symbols used is equal to or larger than standard uncertainties. Solid line = best fit to our data; dotted line = best fit to Angeletti et al. (1977) data: the two trends are parallel with the same slope (0.022). Dashed line = *a* values calculated for the $MgAl_2O_4$-$CoAl_2O_4$ solid-solution series at inversion zero using cation-to-oxygen distances refined in Bosi et al. (2012, this issue).

respect to the starting reagents (Fig. 5). This behavior may be tentatively explained by considering that partitioning of transition element cations between minerals and coexisting melt is strongly influenced by crystal field stabilization energies (CFSE). As for example, in several silicate systems a relationship between CFSE and distribution coefficients has been demonstrated for transition metal ions (Leeman and Scheidegger 1977; Takahashi 1978). The latter authors showed that the partition coefficient (toward crystals) between olivine and silicate groundmass follows the sequence Co > Fe > Mn, that is exactly what is predicted on the basis of CFSE and observed in Figure 5 for spinels. However, CFSE contributes less than 10% to the total lattice energy (Burns 1993), so that other factors must have a larger influence on cation partitioning. According to Goldschmidt's rules, when two different ions occupy a particular position in a crystal structure, the ion with the higher ionic potential forms a stronger bond with anions. In this light the behavior observed in Figure 5 may be easily explained bearing in mind that Co^{2+}, Fe^{2+}, and Mn^{2+} essentially occupy the tetrahedrally coordinated site of the spinel structure and their ionic potential is ranked $^{T}Co^{2+} > {}^{T}Fe^{2+} > {}^{T}Mn^{2+}$.

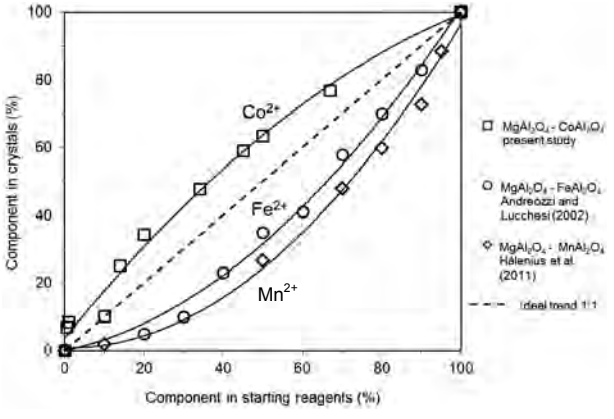

FIGURE 5. Comparison (in terms of chemical components expressed in mol%) between crystal products and starting reagents along the solid-solution series $MgAl_2O_4$-AAl_2O_4 (with A = Co^{2+}, Fe^{2+}, and Mn^{2+}). Continuous lines = best fit to experimental data; dashed line = 1:1 ideal trend.

On the basis of both the above interpretations and results previously obtained (Hålenius et al. 2010, 2011; Bosi et al. 2011), it seems that, better than electronic interactions, steric factors (e.g., size of the ions) are central to determine the cation intra-crystalline distribution in the aluminate spinel structure as well as inter-crystalline partitioning between aluminate spinels and other phases.

ACKNOWLEDGMENTS

The present work benefited from financial support of the Italian PRIN 2008 "SPIN GEO-TECH". Chemical analyses were carried out with the kind assistance of M. Serracino to whom the authors express their gratitude. The review of two anonymous referees and handling of Alexandra Friedrich is acknowledged.

REFERENCES CITED

Andreozzi, G.B. and Lucchesi, S. (2002) Intersite distribution of Fe^{2+} and Mg in the spinel (sensu stricto)- hercynite series by single-crystal X-ray diffraction. American Mineralogist, 87, 1113–1120.

Andreozzi, G.B. and Princivalle, F. (2002) Kinetics of cation ordering in synthetic $MgAl_2O_4$ spinel. American Mineralogist, 87, 838–844.

Andreozzi, G.B., Princivalle, F., Skogby, H., and Della Giusta, A. (2000) Cation ordering and structural variations with temperature in $MgAl_2O_4$ spinel: an X-ray single crystal study. American Mineralogist, 85, 1164–1171.

Andreozzi, G.B., Lucchesi, S., Skogby, H., and Della Giusta, A. (2001) Compositional dependence of cation distribution in some synthetic $(Mg,Zn)(Al,Fe^{3+})_2O_4$ spinels. European Journal of Mineralogy, 13, 391–402.

Angeletti, C., Pepe, F., and Porta, P. (1977) Structure and Catalytic Activity of $Co_xMg_{1-x}Al_2O_4$ spinel solid solutions. Part 1.–Cation distribution of Co^{2+} ions. Journal of the Chemical Society, Faraday Transactions, 1, 73, 1972–1982.

Areán, C.O., Mentruit, M.P., Platero, E.E., i Xamena, F.X.L., and Parra, J.B. (1999) Sol–gel method for preparing high surface area $CoAl_2O_4$ and Al_2O_3-$CoAl_2O_4$ spinels. Materials Letters, 39, 22–27.

Bosi, F., Andreozzi, G.B., Ferrini, V., and Lucchesi, S. (2004) Behavior of cation vacancy in kenotetrahedral Cr-spinels from Albanian eastern belt ophiolites. American Mineralogist, 89, 1367–1373.

Bosi, F., Hålenius, U., Andreozzi, G.B., Skogby, H., and Lucchesi, S. (2007) Structural refinement and crystal chemistry of Mn-doped spinel: A case for tetrahedrally coordinated Mn^{3+} in an oxygen-based structure. American Mineralogist, 92, 27–33.

Bosi, F., Andreozzi, G.B., Hålenius, U., and Skogby, H. (2011) Zn-O tetrahedral bond length variations in normal spinel oxides. American Mineralogist, 96, 594–598.

Bosi, F., Hålenius, U., D'Ippolito, V., and Andreozzi, G.B. (2012) Blue spinel crystals in the $MgAl_2O_4$-$CoAl_2O_4$ series: Part II. Cation ordering over short-range and long-range scales. American Mineralogist, 97, 1834–1840.

Burns, R.G. (1993) Mineralogical Applications of Crystal Field Theory, 2nd ed. Cambridge, University Press, U.K.

Chemlal, S., Larbot, A., Persin, M., Sarrazin, J., Sghyar, M., and Rafiq, M. (2000) Cobalt spinel $CoAl_2O_4$ via sol-gel process: elaboration and surface properties. Materials Research Bulletin, 35, 2515–2523.

Chen, Z.Z., Shi, E.W., Zheng, Y.Q., Xiao, B., and Zhuang, J.Y. (2003) Hydrothermal synthesis of nanosized $CoAl_2O_4$ on $ZnAl_2O_4$ seed crystallites. Journal of the American Ceramic Society, 86, 1058–1060.

Cho, W.S. and Kakihana, M.J. (1999) Crystallization of ceramic pigment $CoAl_2O_4$ nanocrystals from Co–Al metal organic precursor. Alloys and Compounds, 287, 87–90.

Chokkaram, S., Srinivasan, R., Milburn, D.R., and Davis, B.H. (1997) Conversion of 2-octanol over nickel-alumina, cobalt-alumina, and alumina catalysts. Journal of Molecular Catalysis A: Chemical, 121, 157–169.

Eppler, R. and Eppler, D. (2000) Glazes and Glass Coating. The American Ceramic Society, Westerville, Ohio.

Fernández, A.L. and Pablo, L.d. (2002) Formation and the colour development in cobalt spinel pigments. Pigment & Resin Technology, 31, 350–356(7).

Fierro, G., Lo Jacono, M., Dragone, R., Ferraris, G., Andreozzi, G.B., and Graziani, G. (2005) Fe-Zn manganite spinels and their carbonate precursors: preparation, characterization and catalytic activity. Applied Catalysis B: Environmental, 57, 153–165.

Gama, L., Ribeiro, M.A., Barros, B.S., Kiminami, R.H.A., Weber, I.T., and Costa, A.C.F.M. (2009) Synthesis and characterization of the $NiAl_2O_4$, $CoAl_2O_4$ and

$ZnAl_2O_4$ spinels by the polymeric precursors method. Journal of Alloys and Compounds, 483, 453–455.

Guo, J., Griffin, W.L., and O'Reilly, S.Y. (1994) A cobalt-rich spinel inclusion in a sapphire from Bo Ploi, Thailand. Mineralogical Magazine, 58, 247–258.

Hålenius, U., Skogby, H., and Andreozzi, G.B. (2002) Influence of cation distribution on the optical absorption spectra of Fe^{3+}-bearing spinel s.s.-hercynite crystals: evidence for electronic transitions in $^{VI}Fe^{2+}$-$^{VI}Fe^{3+}$ clusters. Physics and Chemistry of Minerals, 29, 319–330.

Hålenius, U., Andreozzi, G.B., and Skogby, H. (2010) Structural relaxation around Cr^{3+} and the red-green color change in the spinel (sensu stricto)-magnesiochromite ($MgAl_2O_4$-$MgCr_2O_4$) and gahnite-zincochromite ($ZnAl_2O_4$-$ZnCr_2O_4$) solid-solution series. American Mineralogist, 95, 456–462.

Hålenius, U., Bosi, F., and Skogby, H. (2011) A first record of strong structural relaxation of TO_4 tetrahedra in a spinel solid solution. American Mineralogist, 96, 617–622.

Harrison, R.J., Redfern, S.A.T., and O'Neill, H.St.C. (1998) The temperature dependence of the cation distribution in synthetic hercynite ($FeAl_2O_4$) from in-situ neutron diffraction refinements. American Mineralogist, 83, 1092–1099.

Hou, Z. and Yashima, T. (2004) Supported Co catalysts for methane reforming with CO_2. Chemistry and Materials Science, 81, 153–159.

Kurajica, S., Tkalčec, E., Gržeta, B., Iveković, D., Mandić, V., Popović, J., and Kranzelić, D. (2011) Evolution of structural and optical properties in the course of thermal evolution of sol–gel derived cobalt-doped gahnite. Journal of Alloys and Compounds, 509, 3223–3228.

Lavina, B., Salviulo, G., and Della Giusta, A. (2002) Cation distribution and structure modeling of spinel solid solutions. Physics and Chemistry of Minerals, 29, 10–18.

Leeman, W.P. and Scheidegger, K.F. (1977) Olivine/liquid distribution coefficients and a test for crystal-liquid equilibrium. Earth and Planetary Science Letters, 35, 247–257.

Li, W., Li, J., and Guo, J. (2003) Synthesis and characterization of nanocrystalline $CoAl_2O_4$ spinel powder by low temperature combustion. Journal of the European Ceramic Society, 23, 2289–2295.

Maljuk, A., Tsurkan, V., Zestrea, V., Zaharko, O., Cervellino, A., Loidl, A., and Argyriou, D.N. (2009) Floating-zone growth of large high-quality $CoAl_2O_4$ single crystals. Journal of Crystal Growth, 311, 3997–4000.

Melo, D.M.A., Cunha, J.D., Fernandes, J.D.G., Bernardi, M.I., Melo, M.A.F., and Martinelli, A.E. (2003) Evaluation of $CoAl_2O_4$ as ceramic pigments. Materials Research Bulletin, 38, 1559–1564.

Mimani, T. and Ghosh, S. (2000) Combustion synthesis of cobalt pigments: Blue and pink. Current Science, 78, 892–896.

Mindru, I., Marinescu, G., Gingasu, D., Patron, L., Ghica, C., and Giuginca, M. (2010) Blue $CoAl_2O_4$ spinel *via* complexation method. Materials Chemistry and Physics, 122, 491–497.

Nakatsuka, A., Ikeda, Y., Yamasaki, Y., Nakayama, N., and Mizota, T. (2003) Cation distribution and bond lengths in $CoAl_2O_4$ spinel. Solid State Communications, 128, 85–90.

O'Neill, H.St.C. and Dollase, W.A. (1994) Crystal structures and cation distributions in simple spinels from powder XRD structural refinements: $MgCr_2O_4$, $ZnCr_2O_4$, Fe_3O_4 and the temperature dependence of the cation distribution in $ZnAl_2O_4$. Physics and Chemistry of Minerals, 20, 541–555.

O'Neill, H.St.C. and Navrotsky, A. (1984) Cation distribution and thermodynamic properties of binary spinel solid solutions. American Mineralogist, 69, 733–753.

Quintiliani, M., Andreozzi, G.B., and Skogby, H. (2011) Synthesis and Mössbauer characterization of $Fe_{1+x}Cr_{2-x}O_4$ ($0 \le x \le 2/3$) spinel single crystals. Periodico di Mineralogia, 80, 39–55.

Rangappa, D., Ohara, S., Naka, T., Kondo, A., Ishii, M., and Adschiri, T. (2007) Synthesis and organic modification of $CoAl_2O_4$ nanocrystals under supercritical water conditions. Journal of Materials Chemistry, 17, 4426–4429.

Sales, M., Valentin, C., and Alarcon, J. (1997) Cobalt aluminate spinel-mullite composites synthesized by sol-gel method. Journal of the European Ceramic Society, 17, 41–47.

Shigley, J.E. and Stockton, C.M. (1984) Cobalt-blue gem spinels. Gems & Gemology, 1, 34–41.

Suzuki, T., Nagai, H., Nohara, M., and Takagi, H.J. (2007) Melting of antiferromagnetic ordering in spinel oxide $CoAl_2O_4$. Journal of Physics: Condensed Matter, 19, 145265.

Takahashi, E. (1978) Partitioning of Ni^{2+}, Co^{2+}, Fe^{2+}, Mn^{2+} and Mg^{2+} between olivine and silicate melts: compositional dependence of partition coefficient. Geochimica et Cosmochimica Acta, 42, 1829–1844.

Taran, M.N., Koch-Müller, M., and Feenstra, A. (2009) Optical spectroscopic study of tetrahedrally coordinated Co^{2+} in natural spinel and staurolite at different temperatures and pressures. American Mineralogist, 94, 1647–1652.

Tielens, F., Calatayud, M., Franco, R., Recio, J.M., Pérez-Ramírez, J., and Minot, C. (2006) Study of the structural and electronic properties of bulk $CoAl_2O_4$ spinel. The Journal of Physical Chemistry B, 110, 988–995.

Tielens, F., Calatayud, M., Franco, R., Recio, J.M., Pérez-Ramírez, J., and Minot, C. (2009) Theoretical investigation of the inversion parameter in $Co_{3-s}Al_sO_4$ (s=0–3) spinel structures. Solid State Ionics, 180, 1011–1016.

Tristan, N., Hemberger, J., Krimmel, A., Krug Von Nidda, H.A., Tsurkan, V., and Loidl, A. (2005) Geometric frustration in the cubic spinels MAl_2O_4 (M = Co, Fe and Mn). Physical Review B, 72, 174404.

Wang, C., Liu, S., Liu, L., and Bai, X. (2006) Synthesis of cobalt–aluminate spinels via glycine chelated precursors. Materials Chemistry and Physics, 96, 361–370.

Manuscript received February 22, 2012
Manuscript accepted July 19, 2012
Manuscript handled by Alexandra Friedrich